Proceedings of the 12th Annual British Columbia Mine Reclamation Symposium in Vernon, BC, 1988.
The Technical and Research Committee on Reclamation

THE APPLICATION OF SPACRBORNE REMOTE SENSING TO EXPLORATION GEOLOGY

by
J. S. MacDonald
June 2, 1988

MINING RECLAMATION SYMPOSIUM, VERNON, BRITISH COLUMBIA

1. INTRODUCTION

High resolution sensing of the earth's surface from orbiting spacecraft began in the early 1970's with the launch of the U.S. LANDSAT series of satellites, in recent years, other satellite systems have been launched which have increased our ability to monitor the surface of the planet and begin to interpret the resulting data in terms of what is indicated about the location and status of its resources. More sophisticated systems are planned for the next decade, and current trends point to the development of remote sensing technology as a powerful information gathering tool which will be used operationally in establishing and maintaining a worldwide resource data base by the turn of the century. This paper examines some of the basic principles behind the use of spaceborne remote sensing as it applies to exploration geology.

2. SENSING THE EARTH FROM SPACE

Before examining the particular application of exploration geology, it is necessary to describe the nature o the measurements which are made from space. Instruments carried on-board earth sensing spacecraft consist mainly of imaging radiometers which generate a set of images of the earth, each of which is composed of rows of measurements of the radiance in a specified region of the electromagnetic specturm across a swath of the earth beneath the satellite. By way of example, the multispectral scanner (MSS) carried on four separate LANDSAT satellites since 1972 simultaneously produces images in four such spectral bands in the visible and near infrared portion of the spectrum. It transmits to earth, four separate images, each of which is a view of the earth in a different region of the spectrum. Figure 1 shows schematically how the MSS sensor is configured. The spatial resolution of an imaging sensor such as the MSS is characterized by the instantaneous field of view (IFOV) which defines the patch on the earth's surface viewed by the sensor at any one instant. Typical IFOVs range from 800 meters for the HRPT system on NOAA-8 to 10 meters for the Panchromatic linear array (PLA) carried on SPOT-1.

All of these instruments must view the earth's surface through its atmosphere. The atmosphere is far from a transparent medium at all wavelengths. Figure 2 shows a curve of atmospheric transmission as a function of wavelength. The various regions of high atmospheric absorption are obvious. The curve of Figure 2 also delineates the various "windows" in the atmospheric absorption spectrum which are useful for sensing the earth's surface from space. These windows are listed in Table 1, and range from ultra-violet through the microwave region of the spectrum. They define the regions of the spectrum which are useful for viewing the earth's surface from space. The regions between the windows are populated by the absorption features of atmospheric gases such as water vapour, O_2 CO_2, etc. and are used in some cases to measure atmospheric characteristics which influence the earth's weather. Examples of this are the water-vapour imaging channel carried on the METEOSAT and GOES satellites and the TIROS Operational Vertical Sounder (TOVS) carried on the NOAA satellite, which operates on the edges of some atmospheric absorption bands. The SPOT satellite also affords the capability to create stereo views of the earth's surface.

3. SENSIMG SYSTEMS

The sensing instruments flown thus far can *be* divided into two types: imaging radiometers, and synthetic aperture imaging radars. Imaging radiometers have been flown covering most useable regions of the spectrum. They are devices which passively sense radiation from the earth and construct images from that data. The mutlispectral scanner displayed in Figure 1 is typical of such an instrument. Synthetic Aperture Radar, on the other hand, is an active sensor which radiates pulses of microwave energy toward the earth and measures the reflected return, forming an image which describes the microwave reflectivity and backscatter from the earth's surface. Table 2 lists the spectral regions covered and the IFOV of the more important earth sensing satellite instruments which have flown up to this time.

4. THE APPLICATION OF SPACEBORME SEMSING TO EXPLORATION GEOLOGY

There are three broad approaches to the use of spaceborne sensing instruments in exploring for minerals. The first of these *is* direct sensing of substances on the earth's surface which are indicators of mineralization. This approach requires that there be little or no vegetative cover in the region, and is useful in arid areas such as the Great Basin of the western United States and many other similar areas of the world.

The second approach involves indirect sensing of potential mineralization throughits influence on plant life in a vegetated region, or through measurement of the thermal inertia of formations within a region. The geobotanical approach divides into two main classes: The detection of vegetation species preferences related to solid minerals (indicator geobotany), and the detection of plant stress caused by mineral content in the soil.

The third approach involves determination of surface structure from spaceborne images. Images of the earth from orbital altitude, because they cover a wide area, reveal features such as faults, etc., which are not apparent from lower altitude imagery. Synthetic Aperture Radar (SAR) is particularly effective in this respect since it exploits the acute sensitivity of that instrument to surface roughness and surface orientation. There has been one instance reported of the ability of L-band SAR to penetrate hyper-dry surface sand, revealing subterranean structure (McCauley et al, 1982). However, this is a very special case which relies on the ability of long wavelength radar to penetrate hyper-arid soils.

5. DIRECT SENSING OF GEOLOGICAL MATERIALS

The direct sensing and identification of surface materials depends on the detection of spectral features such as absorption bands which are diagnostic of particular materials. The VIS, SWIR and TIR windows all have significant features present. These are summarized in Table 3.

Figure 3 is illustrative of the basic spectral properties which are useful in the mapping of hydrothermal alteration from space in non-vegetated areas. Shown here are the spectral reflectance curves for unaltered quartz latite in the VIS, NIR and SWIR spectral windows. In latite (heavy line, Figure 3), note the marked fall-off from 0.7 to 0.45 um and the broad absorption band in the 0.8 to 0.95 um region. In contrast, the spectra for the equivalent unaltered rock show a very gradual increase in reflectivity up to approximately 1.2um. The higher altered latite spectrum result from the oxidation of iron sulfide process yields the obvious absorption features at 2.2 um and 2.35 um. These spectral changes characterize the results derived from supergene weather of hydrothermally altered rock.

Examination of Figure 3 reveals that by simply taking the ratio of various Thematic Mapper (TM) bands, it is possible to discriminate between altered and unaltered rock. For example, the ratios of band 5 to 7 and 5 to 4 will both show a lighter response in regions of altered rock than in unaltered regions. Interpreations of such ratio images must be done in the context of other knowledge of the geology of the region, but the use of such images provides a powerful tool for the exploration geologist.

An illustration of the use of these techniques in lithologie mapping is provided by the work of Bryan Bailey and his colleagues (Bailey et al, 1982). Their work involved the co-operative assessment of the LANDSAT MSS and TM, the latter instrument being simulated by an airborne scanner (TMS), with respect to their ability to separate lithologie units into two test areas. Band ratioing, principle component analysis and canonical analysis were all carried out on the data to enhance the discrimination of lithologie units within the images. The TMS provided the best discrimination, and the results apear in Figures 4 through 7 for the Split Mountain study area in north-eastern Utah. For purposes of illustration, most rock units in the Split Mountain area can be considered to be composed of one or more of the following lithologies: (a) light colored sandstones, (b) gray shales, and (c) red beds of sandstone, siltstone and shale. Reflectance spectra, in the TMS (Thematic Mapper Simulator) bandpasses, representative of each of these general lithologie groups are shown in Figure 4. Using these spectra, certain rock identifications can be interpreted from the TMS ratio images shown in Figure 5. For the bands 3/2 ratio image, the spectra indicate that red beds should have he brightest response (highest ratio value), sandstones should have *a* bright to intermediate response, and shales should have the darkest response. The same general relationships are also true for the bands 4/2 ratio image. On the bands 6/3 ratio image, the red beds and shales should be relatively dark and the sandstones bright to intermediate. On a color ratio image with ratio 3/2 displayed as red, ratio 4/2 as green, and ratio 6/3 as blue, the red beds are bright orange-yelow, shales are dark purple, and the sandstones range through intermediate to light blueish colors. Further refinement in rock-type identifiation can be achieved by using topographic information obtained from one of the original single band images by examining shadow features. This topographic information permits interpretation of the relative competence of the red beds and identification of them as dominantly shale, siltstone or sandstone. By using these techniques, supplemented by interpretations of both principle components and canonical analysis enhancements of the TMS data, Bailey and his co-workers discriminated the dominant lithologies of the Split Mountain area, and mapped them as shown in Figure 6. This map was prepared from overlay analysis of various enhanced color

composite TMS images. Rock units are not labelled to avoid clutter but general correlation with corresponding units of a geological map of the region (Figure 7) is not difficult. in some instances, discrimination of the rock units on TMS images is even more precise than shown on the detailed geological map of the area. For example, the distribution of Moncos Shale (Kms) exposures just east of the Green River (Section 33) are generalized on the Geological map in Figure 7. However, certain TMS images (figure 5 ratio 4/2)) precisely define the Moncos Shale pattern in this area. A field check confirmed that the Moncos Shale in this area was covered by a thin veneer of gravel and was exposed only in gullies, as suggested by TMS bands 4/2 ratio image, (Bailey, 1982).

6. IMDIRECT SEMSING OF GEOLOGICAL UNITS

The techniques described above work well in areas of zero or very sparse vegetation cover, but what about that much larger part of the earth which is covered by plants? In this case one is forced to attempt to discover the presence of minerals indirectly by examining the plant life itself. Figure 8 shows the reflectance spectra of four representative plants, a shrub, a broad-leafed deciduous tree, a conifer and grass. The major features associated with plant spectra are the steep rise around 0.7 urn and the peak at 0.58 urn. It is this latter feature that causes plants to appear green. Chlorophyll pigments cause strong absorption bands at 0.45 urn and 0.68 urn. in the 0.7 urn to 1.3 urn range, refractive index discontinuities, morphologic and physiologic considerations, and the lack of pigment induced absorption account for the high reflectivity (Gates et al, 1965, Gausman, 1977). The small dips near 0.95 urn and .1.2 urn are evidence of overtones of longer wavelength water absorption bands (Allen and Richardson, 1968).

The use of spectral information related to the plant canopy for exploration geology centers on two basic geobotanical techigues (a) exploiting the preference of certain species of plants for particular soil types (the use of indicator plants), and (b) detecting plants which have been subjected to stress due to metal content in the soils on which they feed.

Although at first glance the curves of Figure 8 seem to indicate that separation of plant species by spectral analysis is relatively straightforward, such is not the case. The differences in reflectance spectra between various plant species can be quite subtle. In addition, some plants produce blooms and go through seasonal cycles, both of which dramatically affect their spectral reflectance characteristics (See Figure 9). in addition, leaf moisture content and density of vegetation also affect the reflectance spectrum in major ways (See Figure 10).

Thus we see that geological interpretation of reflectance spectra from plants must take account of the life cycle of the plant, its environment, the particular background of species with which it is co-located, and the particular characteristics of plants within the region in which exploration is being pursued. It must always be remembered that spaceborne sensing is but one tool of the arsenal of the exploration geologist, and is a supplement to - not a replacement for - his traditional methods.

An example of the usée of indicator plant geobotany is provided by the work of Ted Reimichen (Reimichen, 1982). who used a combination of spaceborne geobotanical remote sensing with geochemical and geophysical analysis to locate a large deposit of gypsum in southeastern British Columbia which has so far proven 100,000,000 tonnes of economic grade gypsum.

While engaged in field work in southeastern British Columbia in 1979, Reimichen noted that a rose coloured perennial herb, commoney termed "moneky-flower" (Mimulus Lewisii) grew in profusion in areas of low value carbonate. Close inspection revealed finely comminuted pieces of gypsum and anhydrite between the soil beds. As a result he concluded that Mimulus Lewisii could be a likely indicator plant for gypsum in that region, although none of the areas of gypsum occurence assocated with Mimulus found during the 1979 field work were of commercial size and grade.

Computer compatible tapes of LANDSAT MSS images of the region for July and August of several years were obtained, and using a computer-based image analysis system, target areas of known occurrences of Mumulus Lewisii were delineated and used as training areas for the computer. The resulting computer classification of the images delineated several areas of similar spectral properties principally upstream of the training areas on both sides of the Lussier River. These proved to be further occurrences of Mimulus Lewisii. Reconnaissance drilling and further geophysical and trenching work proved the occurrence of large quantiies of commercial grade gypsum covered by up to five meters of overburden and one to several meters of limestone beneath several occurrences of Mimulus Lewisii as delineated on the spacecraft images (see Figure 11).

The detection of stressed vegetation is another promising geobotanical exploration technique which has been shown in some cases to be operationally effective, mainly through the work of Bill Collins. The technique used is to detect a subtle shift of the near infrared rise in *a* plant's spectrum when the plant is subjected to some forms of heavy-metal stress (Collins et al, 1983). Figure 12 shows the phenomenon

being exploited by this method. Here, the introduction of copper sulphate causes the near infrared rise to shift toward the blue end of the spectrum. This example is from laboratory experiments, and as Goetz, et al have pointed out (Goetz et al, 1982) it is risky to draw too broad conclusions from such limited data. However, the basic technique has been shown to yield extremely encouraging results in airborne overflights of known metal-stressed coniferous forest canopies as shown in Figure 13 (Collins, et al 1983), in addition to which similar results have been obtained for mixed deciduous forest canopies on mineralized sites (Milton, et al 1983). The fact that the blue shift phenomenon can be demonstrated in both broadleaf forest species and coniferous forest species strongly suggests a relatively universal pigment response on the part of green plants to specific types of geochemical stress.

It is interesting to note (Collins, et al 1983) that the blue shift was not detected over iron sulphide zones, whereas it was detected over lead and copper sulphide zones. These data are consistent with the competition inhibition model of selective ion uptake in the root zone for explaining heavy metal toxicity and may well provide information useful in interpreting the true botanical nature of the blue shift. Further evidence which lends credibility to the inhibition model is the result that high concentrations of copper and zinc alone generate a blue shift, while similar concentrations of copper and zinc in combination with iron and lead do not. (Chang and Collins, 1983). Clearly a good deal more research must be done to fully understand and interpret the blue shift phenomenon before spaceborne systems will be launched which exploit it. There is no doubt, however, that this technique is a powerful one, and will have a significant influence in the design of future satellite based systems.

7. SENSING GEOLOGIC STRUCTURE

Single images of large portions of the earth's surface greater than 10,000 square kilometers in area reveal geological features such as lineaments, faults, fractures, domes, layered rock and outcrops which, because of their size and relationship to one another can only be readily seen on such images. Such features have been observed since 1972 on LANDSAT images, and in the early stages of that program such observations were he basis of the largest part of the geological application of LANDSAT imagery. More recently the SEASAT and Shuttle imaging Radar (SIR-A and SIR-B) flights have yielded high resolution synthetic aperture radar images of the earth's surface. Synthetic aperture radar (SAR) produces an image which is a two dimensional representation of surface scattering of the microwave pulse. This scattering is in turn a function of the surface physical properties such as roughness, slope, orientation and dielectric constant (Sabins, 1978).

Because of its high sensitivity to surface slope and orientation, as well as roughness, SAR is a particularly effective sensing system for revealing surface manifestations of geological structure (see, for example, Elachi, et al, 1982).

Structural features which can readily be mapped from spaceborne imagery are those features which are represented by some physical elements on the earth's surface. These are usually fractures or physical discontinuities in the rock materials. They can be seen because of the effects of differential or selective erosion and are seen in two distinct manners: (1) The linearity of physical features, and (2) The discontinuity of tone, shape, texture, and/or pattern. The linearity of physical features is an important clue to structure because such linearity occurs from selected erosion along planes of weakness (joints or faults). The discontinuity of tone, shape, texture, or pattern, is created by differential erosion of the terrain on one side of a fracture in preference to the other side. This differential erosion because of differences in rock type, intensity of the natural processes, geomorphic history, and/or types of available geomorphic processes (Cannon, 1982).

Linear features are most visible when they are at right angles to the direction of illumination, in a radar system, one has control over the illumination direction, therefore much can be gained by combining information from more than one direction of radar illumination.

8. FUTURE TRENDS

At the present time, two major satellite systems are functioning: the U.S. LANDSAT system., and the French SPOT system. In addition to this, the Japanese have launched an experimental satellite known as MOS-I (Marine Observation Satellite) and India has recently launched that country's first earth observation satellite IRS-I.

In 1990, the European Space Agency will launch ERS-I. The imaging instrument on this satellite will be a C-Barid (5 GHz) Synthetic Aperture Radar (SAR). This will be followed in 1995 by the Canadian RADARSAT satellite which will also carry a C-Band SAR. This instrument will be much more sophisticated than the one carried on ERS-I, and will have multi-incidence angle capability. It will have an orbit which will allow radar coverage of the arctic regions at less than one day intervals for continuous ice reconnaissance.

A sophisticated earth observation satellite, also named ERS-I, is scheduled for launch by the Japanese in 1991. It will carry an L-Band (1.7 GHz) SAR and a multi-band optical sensor in the VIS, NIR, SWIR and TIR bands which will have a IFOV of 18 meters and stereo capability.

LANDSAT-6 is scheduled for launch in the early 1990's and plans call for the launch of LANDSAT-7 in the middle of the 1990's. Further U.S. plans involve the launching of the Earth Observing System (EOS) in the late 1990's. This system will carry a wide variety of remote sensing instruments, but principal among them will be a multi-frequency synthetic aperture radar with multi-incidence angle and multi-polarization capability, and an imaging spectrometer. Imaging spectrometers are the most advanced imaging instrumens that have yet been conceived for use at optical wavelengths. Such an instrument forms up to 200 individual images, each one measuring approximately 10 nanometers. Thus for each geographic point on the image, a detailed measurement of the spectrum is obtained.

The other important area of development in the use of remote sensing technology *is* in the area of data handling systems, database structures and analysis systems. The development of systems which permit remote sensing measurements from different instruments to be combined and integrated with other types of data describing a geographic area will enable the more extensive utilization of spaceborne earth observation systems in exploration and resource management on an operational scale.

TABLE 1 - ATMOSPHERIC WINDOWS

0.3 µm to 0.4 µm	-	Ultraviolet (UV)
0.4 µm to 0.7 µm	-	Visible (VIS)
0.7 µm to 1.1 µm	-	Near Infrared (NIR)
1.2 µm to 1.3 µm	-	Short wave Infrared (SWIR)
1.5 µm to 1.75 µm	-	Short wave Infrared (SWIR)
2.0 µm to 2.5 µm	-	Short wave Infrared (SWIR)
3.0 µm to 4.2 µm	-	Thermal Infrared (TIR)
8 µm to 14 µm	-	Thermal Infrared (TIR)
0.15 cm to 0.45 cm	-	Microwave
above 0.6 cm	-	Microwave

TABLE 2 - SATELLITE/SENSOR CHARACTERISTICS

SATELLITE	SENSOR	IFOV (M)	BAND NO.	SPECTRAL BAND (μm)
LANDSAT	MULTISPECTRAL SCANNER (MSS)	80	5 6 7 8	0.5 - 0.6 0.6 - 0.7 0.7 - 0.8 0.8 - 1.1
LANDSAT	THERMATIC MAPPER (TM)	30	1 2 3 4 5 7	0.45 - 0.52 0.52 - 0.60 0.63 - 0.69 0.78 - 0.90 1.55 - 1.75 2.08 - 2.35
		120	6	10.40 - 12.58
NOAA 8	AVHRR	1 km	1 2 3 4	0.58 - 0.68 0.725 - 1.10 3.55 - 3.93 10.5 - 11.5
SEASAT	SAR	25 (4 LOOK PROCESSING)	L-BAND	1.27 GH_z
SPOT	MLA	20	1 2 3	0.50 - 0.59 0.61 - 0.68 0.79 - 0.89
	PLA	10	1	0.50 - 0.73
MOS-1	MESSR	50	1 2 3 4	0.51 - 0.59 0.61 - 0.69 0.72 - 0.80 0.80 - 1.1

TABLE 3 - SUMMARY OF SPECTRAL WINDOWS WITH GEOLOGICALLY IMPORTANT SPECTRAL FEATURES.

SPECTRAL WINDOW	MINERAL GROUPS WITH DIAGNOSTIC SPECTRAL FEATURES
0.4 - 1.1 μm	Iron Oxides (limoaite, goethite, hematite)
2.1 - 2.4 μm	Clays and Micas (Kaolinite, Montmourillonite, illite, sercite-muscovite) Sulfates (alunite, gypsum, jarosite) Carbonates (calcite, dolonite)
8.0 - 14.0 μm	Silica (jasperoid, chalcedony, opal, chert) Background Silicates (full compositional range from basalt to rhyolite to quartzase sandstone) Carbonates, clays, sulfates

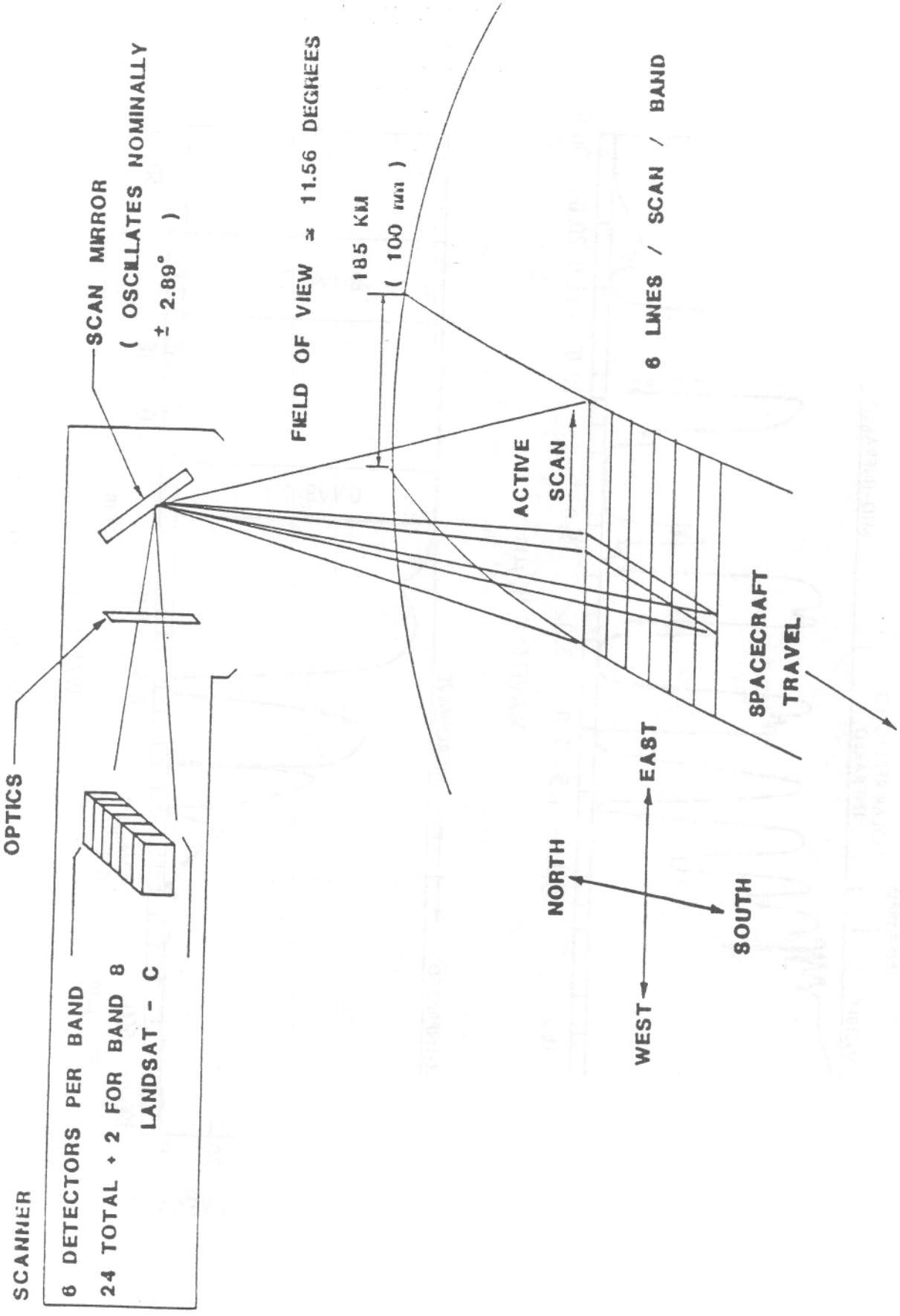

FIGURE 1 LANDSAT MSS SCANNING ARRANGEMENT

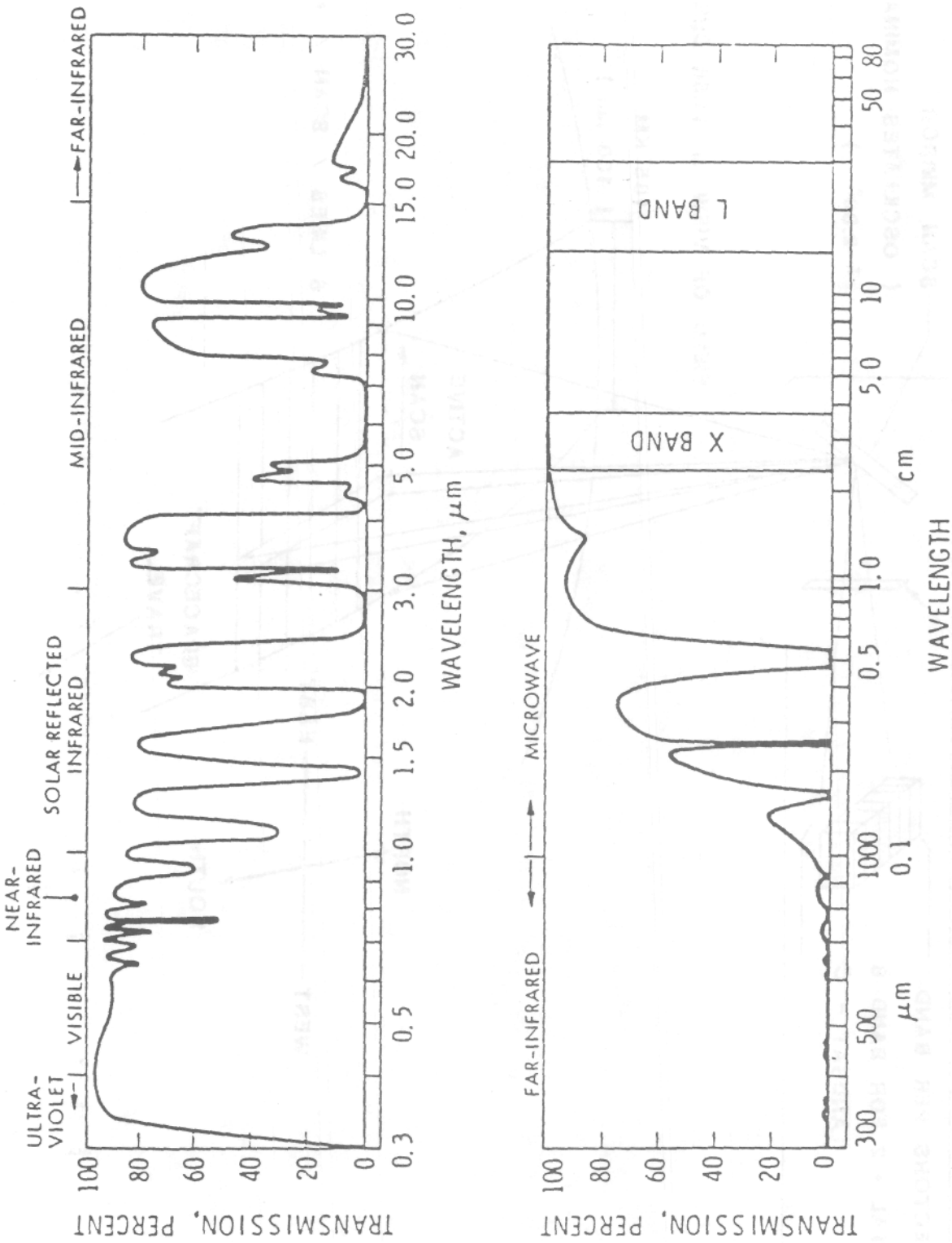

FIGURE 2 ATMOSPHERIC TRANSMISSION

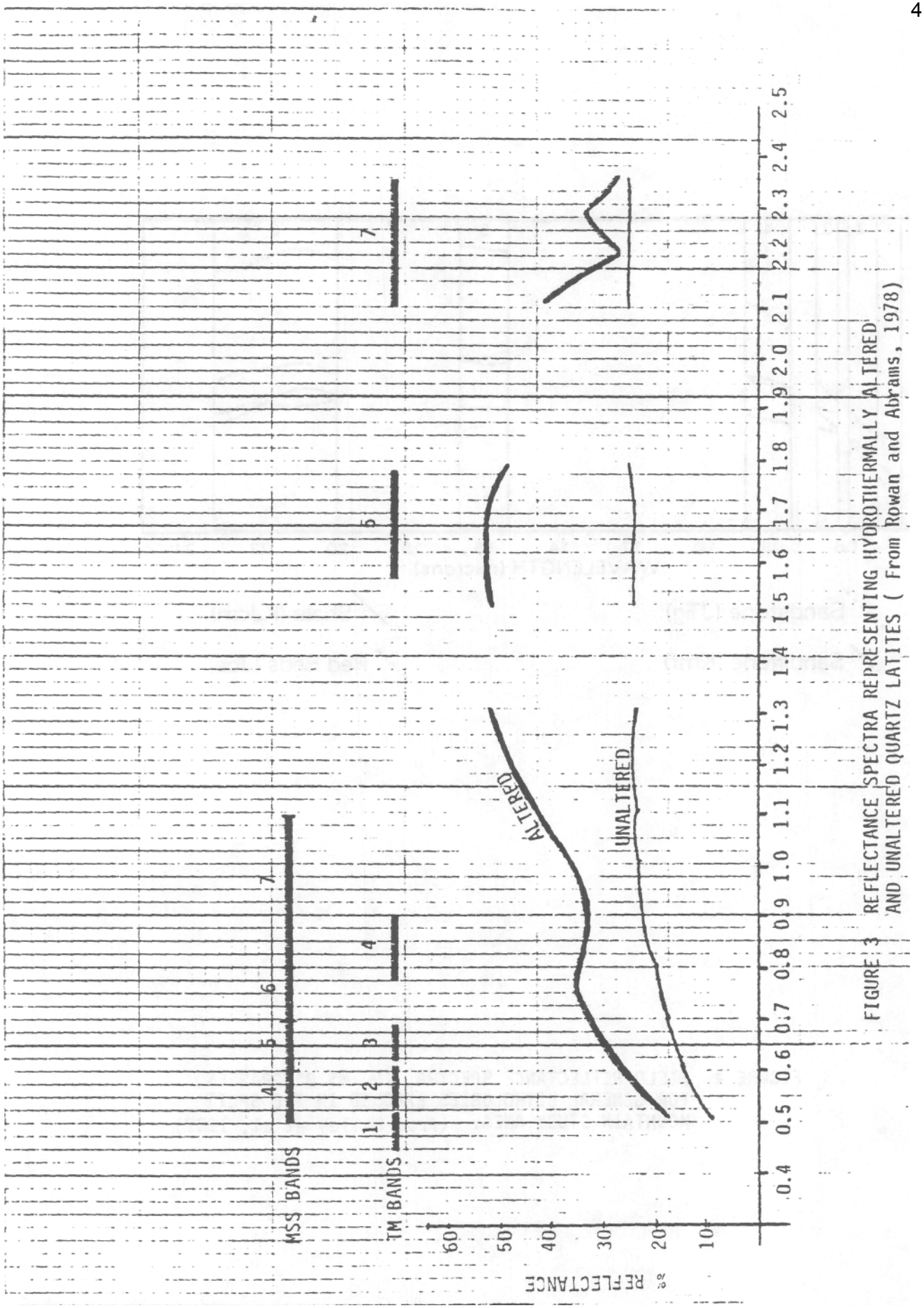

FIGURE 3 REFLECTANCE SPECTRA REPRESENTING HYDROTHERMALLY ALTERED AND UNALTERED QUARTZ LATITES (From Rowan and Abrams, 1978)

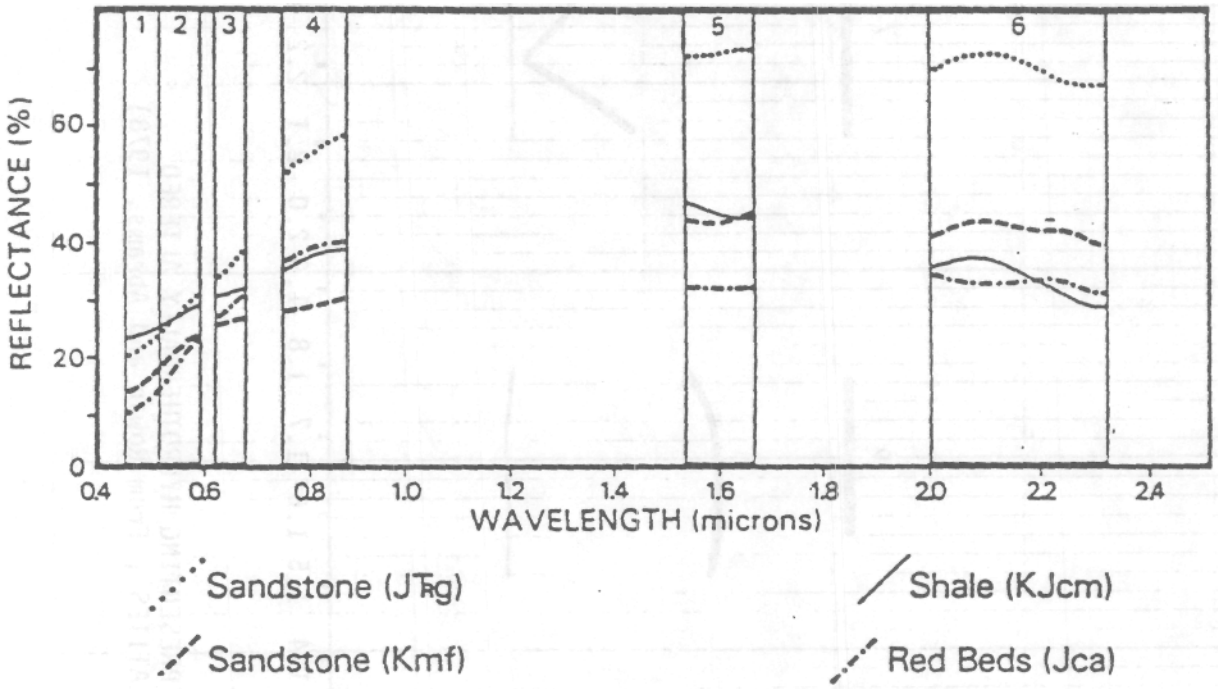

FIGURE 4 FIELD REFLECTIANCE SPECTRA, IN TMS BANDPASSES, FOR GENERAL LITHOLOGIES EXPOSED IN THE SPLIT MOUNTAIN STUDY AREA. (From Bailey et al, 1982)

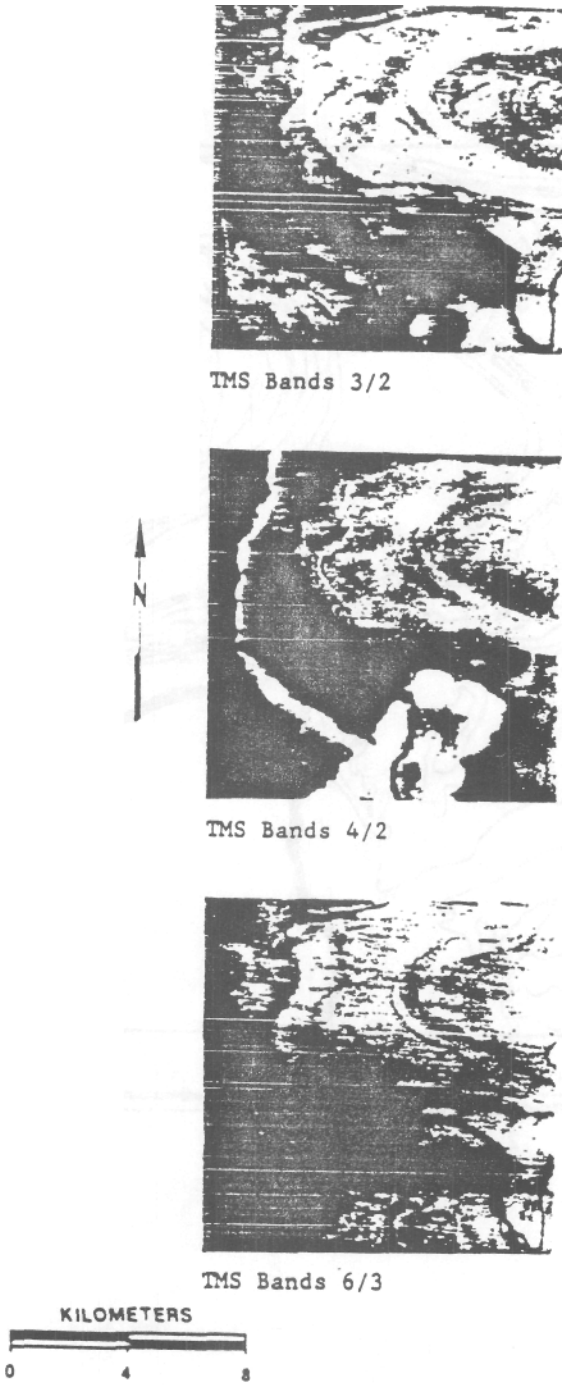

FIGURE 5 MSS AND TMS RATIO IMAGES OF THE SPLIT MOUNTAIN STUDY AREA. (From Bailey et al, 1982)

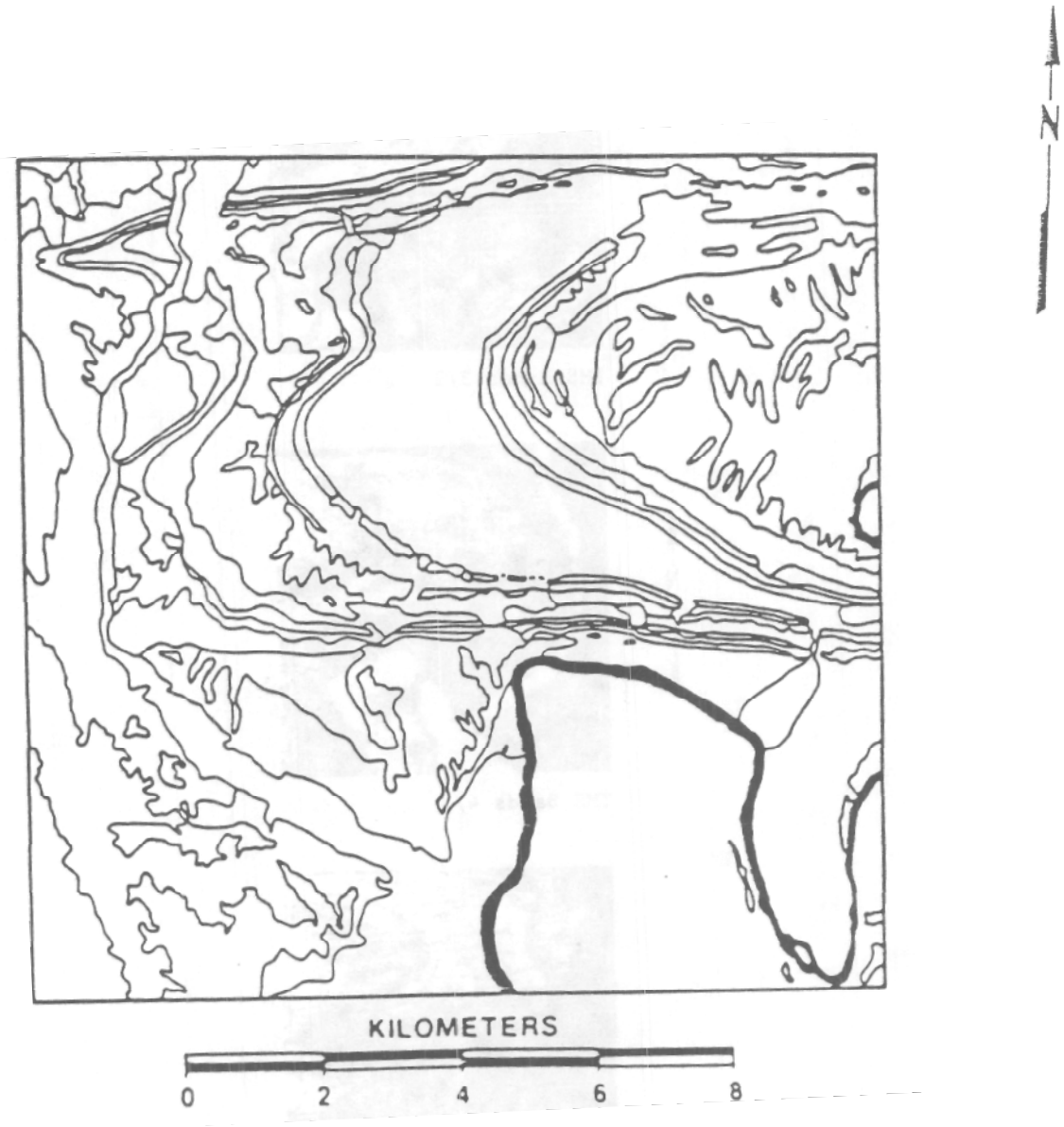

FIGURE 6 MAP SHOWING RESULTS OF LITHOLOGIC DISCRIMINATION FROM ENHANCED TMS IMAGES OF THE SPLIT **MOUNTAIN** STUDY AREA. (From Bailey et al 1982)

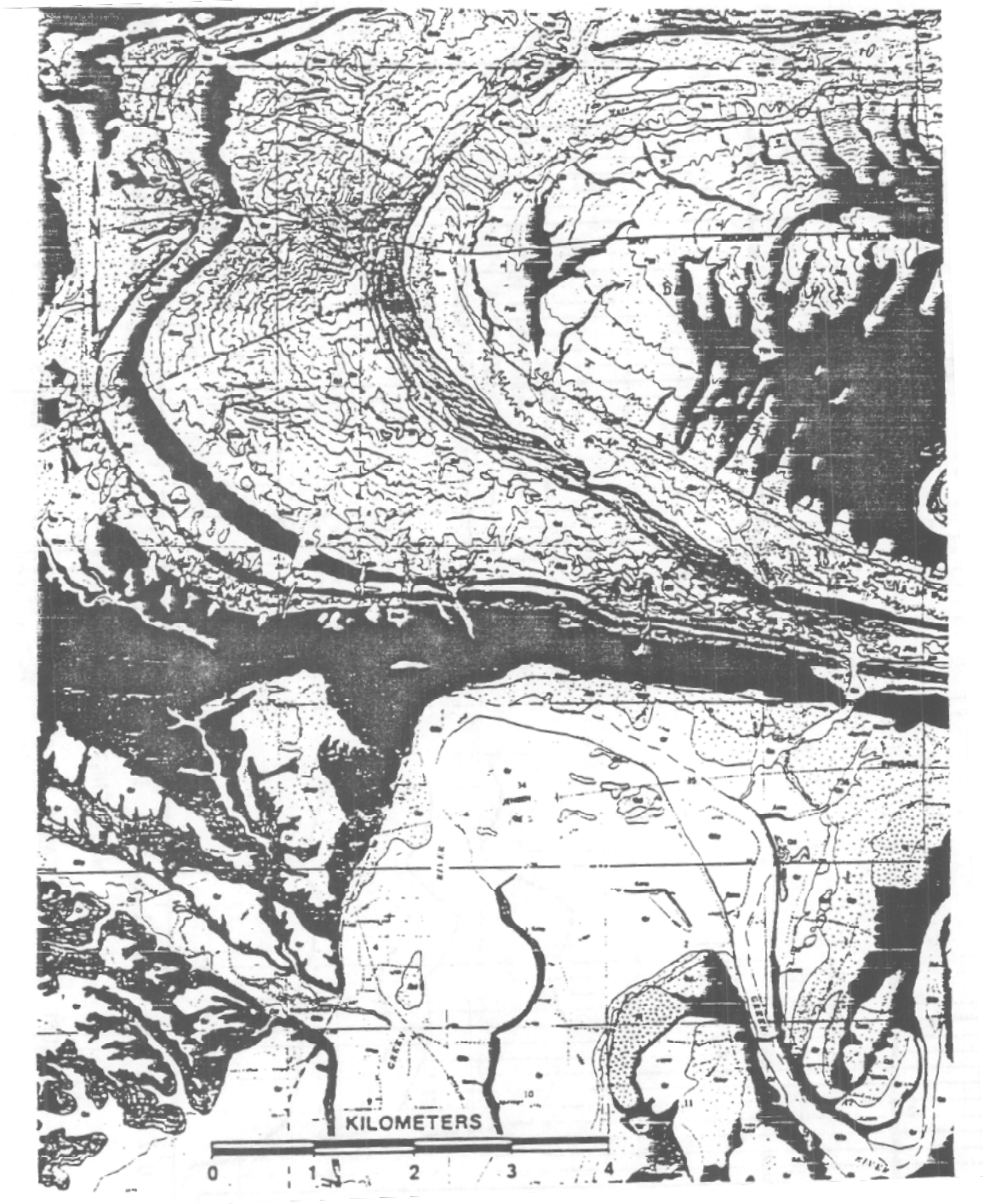

FIGURE 7 DINOSAUR QUARRY 7.5-MINUTE GEOLOGIC MAP (ROWLEY AND OTHERS 1979) CORRESPONDING TO A PORTION OF THE SPLIT MOUNTAIN STUDY AREA. (From Bailey et al, 1982)

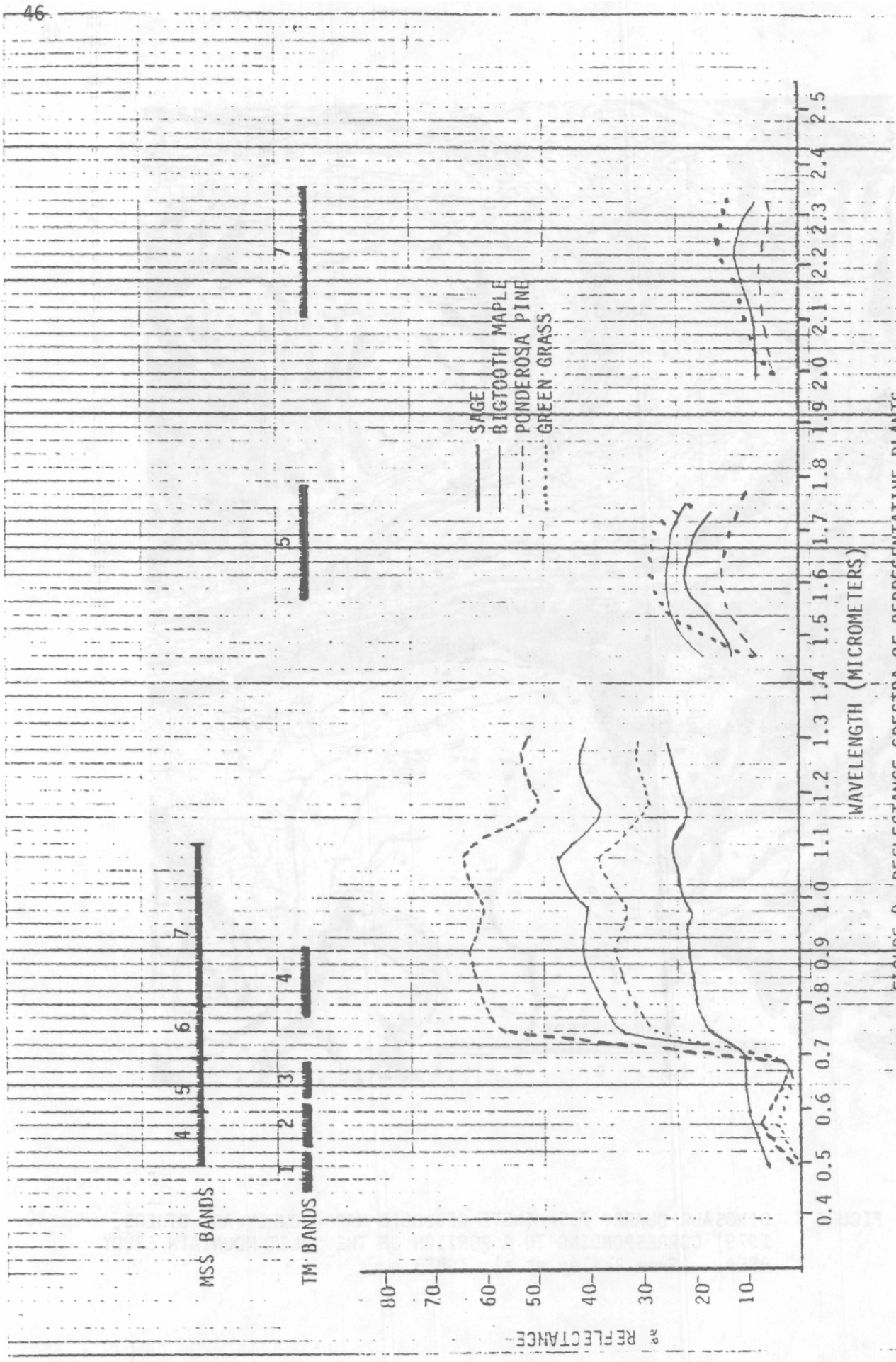
SAGE
BIGTOOTH MAPLE
PONDEROSA PINE
GREEN GRASS
WAVELENGTH (MICROMETERS)
% REFLECTANCE
MSS BANDS
TM BANDS

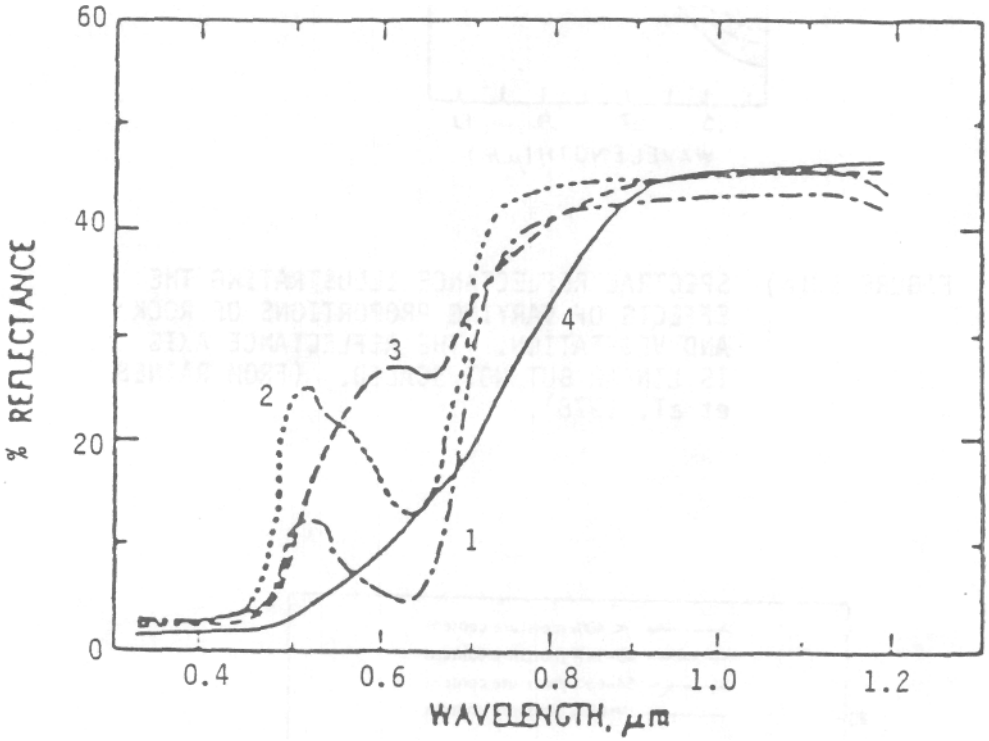

FIGURE 9 REFLECTANCE SPECTRA FOR A HEALTHY BEECH LEAF (1) AND BEECH LEAVES IN PROGRESSIVE PHASES OF SENESCENCE (2-4) (FROM KNIPLING, 1969).

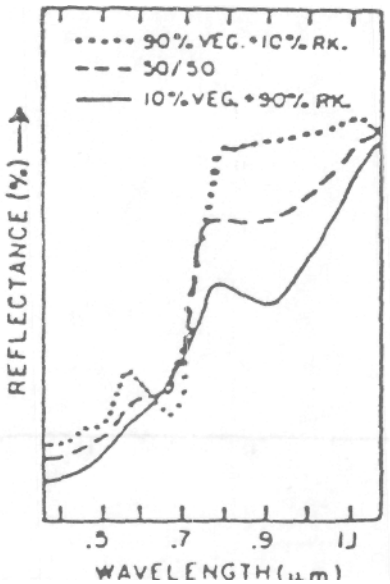

FIGURE 10(a) SPECTRAL REFLECTANCE ILLUSTRATING THE EFFECTS OF VARYING PROPORTIONS OF ROCK AND VEGETATION. THE REFLECTANCE AXIS IS LINEAR BUT NOT SCALED. (FROM RAINES et al. 1978).

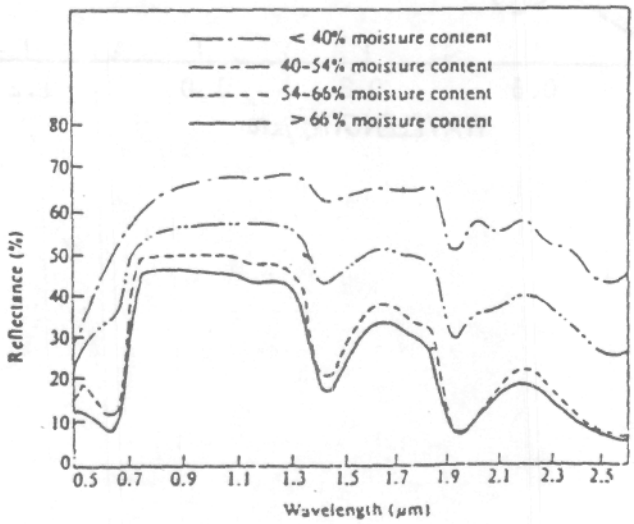

FIGURE 10(b) SPECTRAL CURVES REPRESENTING LEAVES OF VARIOUS MOISTURE CONTENTS. REFLECTANCE DATA FOR CORN LEAVES (AFTER HOFFER AND JOHANNSEN, 1969)

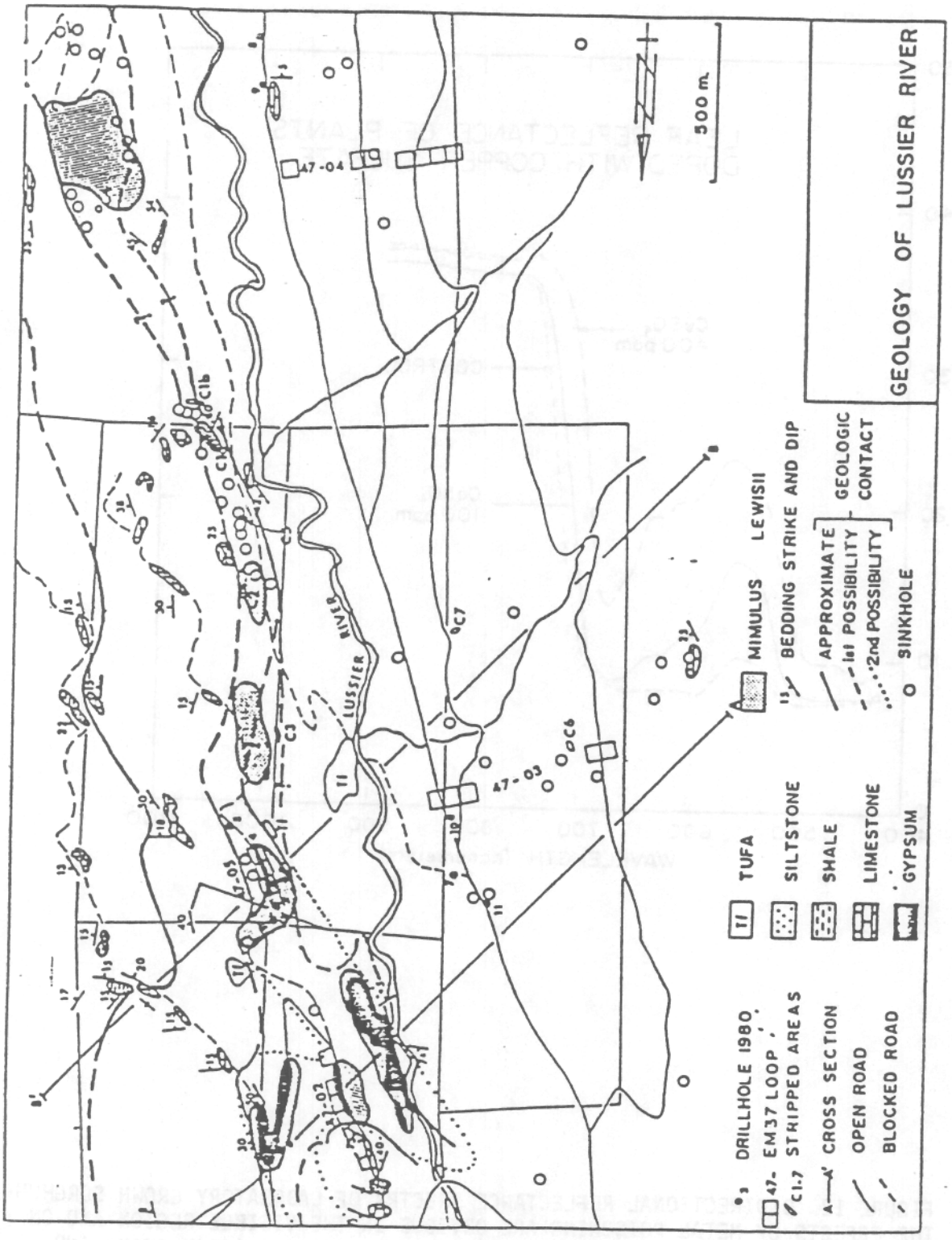

FIGURE 11 GEOLOGY OF THE LUSSIER RIVER AREA (FROM REIMCHEN, 1982)

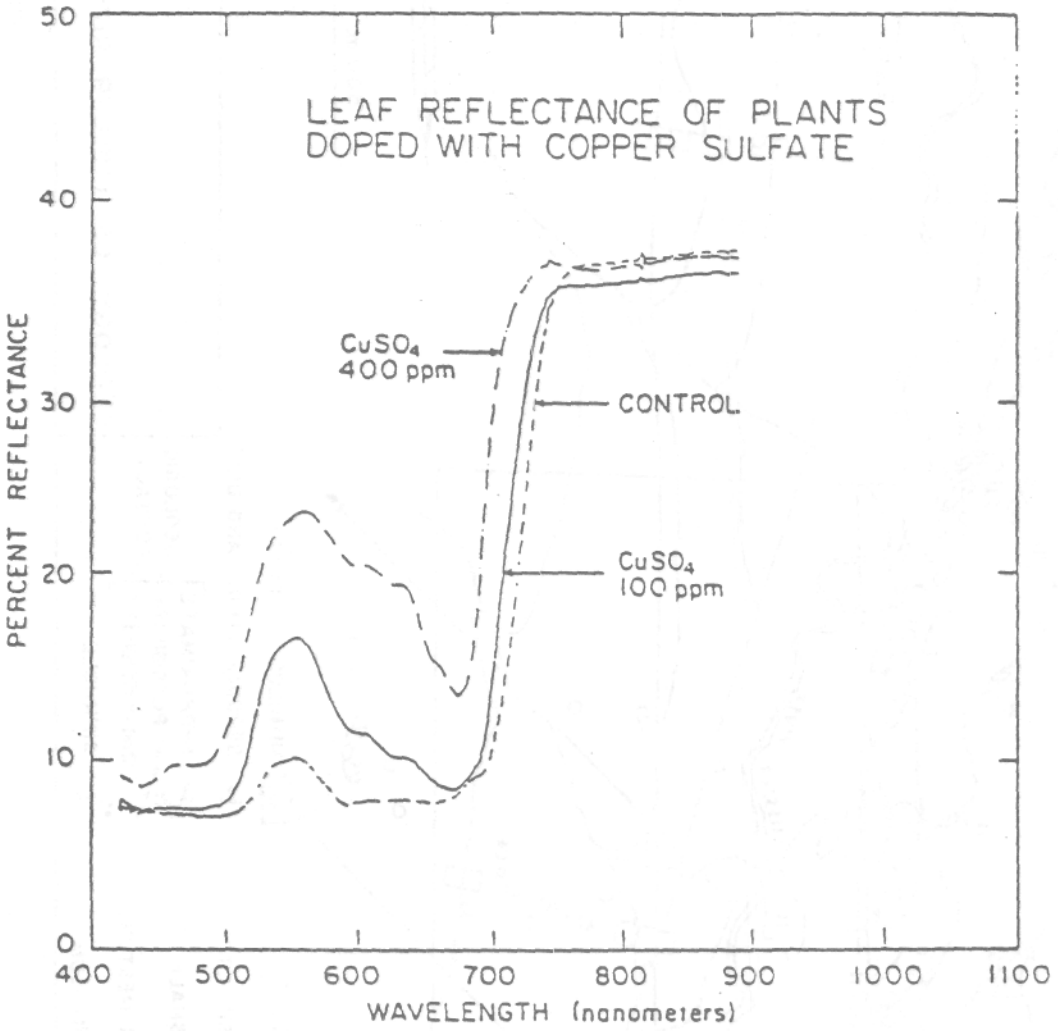

FIGURE 12 BIDIRECTIONAL REFLECTANCE SPECTRA OF LABORATORY GROWN SORGHUM THE EFFECTS OF METAL POISONING ARE OBVIOUS IN THE VISIBLE REGION AND ON THE NEAR INFRARED ABSORPTION EDGE AT 700nm TO 750nm. (FROM CHANG AND COLLINS, 1983)

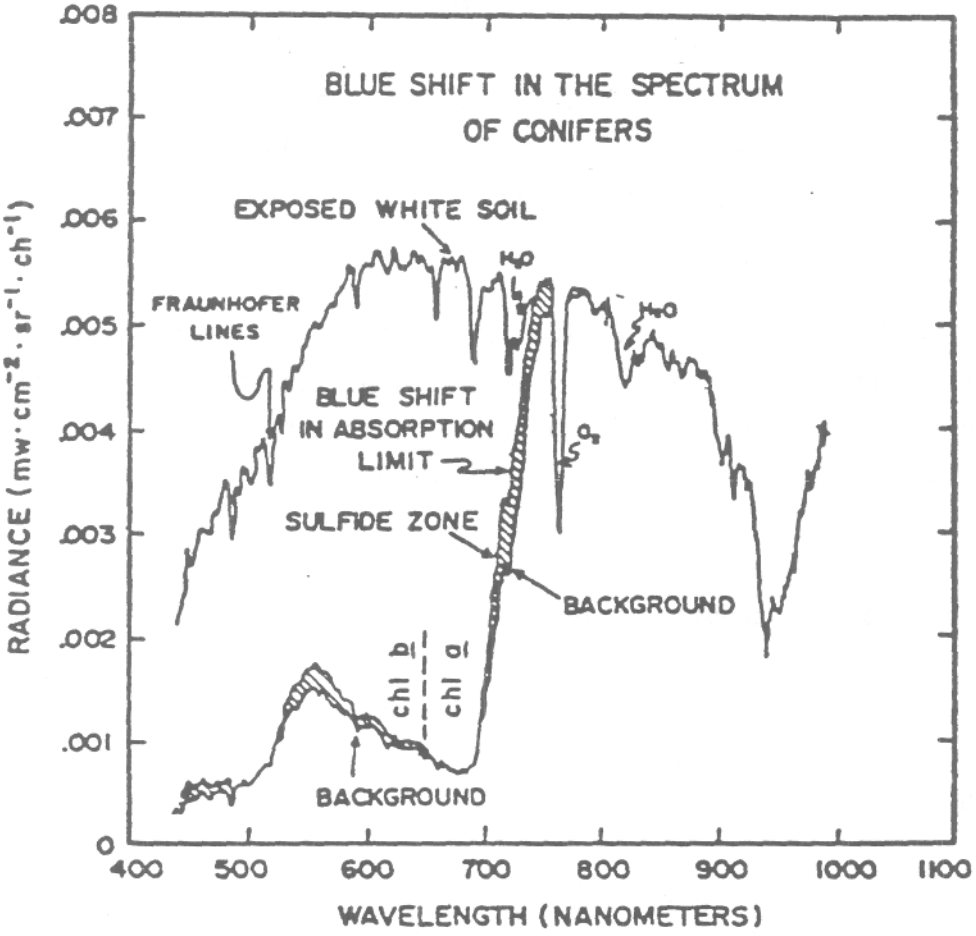

FIGURE 13 AIRCRAFT SURVEY SPECTRA SHOW THE BLUE SHIFT CAUSED BY'MINERAL-INDUCED STRESS IN TREES TOGETHER WITH NORMAL (BACKGROUND) TREE SPECTRA AND THE SPECTRUM OF EXPOSED SOIL. (FROM COLLINS et al, 1983)

REFERENCES

Allen, W. A. and A. J. Richardson, 1968, Interaction of Light on the Plant Canopy, Opt. Soc. of America Journal, Vol. 58, pp. 1023 - 1028

Bailey, G. B., J. R. Francica, J. L. Dwyer, M. S. Feng, 1982, Extraction of Geologic Information from LANDSAT Multispectral Scanner and Thematic Mapper Simulator Data from the Vimta and Piceance Basiss, Utah and Colorado. Proceedings of the International Symposium on Remote Sensing of Environment, Second Thematic Conference, Remote Sensing for Exploration Geology, Fort Worth, Texas, December 1982, pp. 43 - 70

Cannon, P. J., 1982, Quantitative Evaluation of the Information Levels from Radar Imagery for Geologic Exploration. Proceedings, International Symposium on Remote Sensing of Environment, Second Thematic Conference, Remote Sensing for Exploration Geology, Fort Worth, Texas, pp. 355 - 363

Chang, S.-H and W. Collins, 1983, Laboratory Conformation of a Mineral Exploration Technique: Economic Geology, Vol. 78, pp. 723 - 736

Collins, W., S.-H Chang, G. Raines, F. Canney, and R. Ashley, 1983, Airborne Biogeochemical Mapping of Hidden Mineral Deposits: Economic Geology Vol. 78, pp. 737 - 749

Elachi, C., W. E. Braun, J. B. Cimimo, T. Dixon, D. L. Evans, J. P. Ford, R. S. Saunders, C. Breed, H. Masursky, J. F. McCauley, G. Schaber, L. Dellwig, A. England, M. MacDonald, P. Morten-Kaye, F. Sabius: 1982, Shuttle Imaging Radar Experiment, Science, Vol. 218, No. 4576, pp. 996 - 1003

Gates, D. M., H. J. Keegan, J. C. Schleter, and V. R. Weidner, 1965, Spectral Properties of Plants, Applied Optics, Vol.4, pp. 11 - 20

Gausman, H. W., 1977, Reflectance of leaf components: Remote Sensing of Environment, Vol. 3, pp. 1 - 9

Goetz, A. F. H., B. N. Rock and L. C. Rowan, 1983, Remote Sensing for Exploration: An Overview, Economic Geology Vol. 78, pp. 573 - 590

Hoffer, R. M., and C. J. Johannesen, 1969, Ecological Potentials in Spectral Signature Analysis in Johnson, P. L. éd., Remote Sensing in Ecology, Athens, Univ. of Georgia Press, pp. 1-16

Knipling, E. B., 1969, Leaf Reflectance and Image Formation on Color Infrared Film, in Johnson, P. L. éd., Remote Sensing in Ecology: Athens, Univ. of Georgia Press, pp. 17 - 29

McCauley, J. F., G. G. Schaber, C. S. Breed, M. J. Grolier, C. V. Haynes, B. Issaivic, C. Elachi, R. Blom, 1982, Subsurface Valleys and Geoarcheology of the Eastern Sahara Revealed by Shuttle Radar, Science Vol. 218, No. 4576, 3 December 1982 pp. 1004 - 1020

Milton, N. M., W. Collins, S.-H Chang, R. G. Schmidt, 1983, Remote Detection of Metal Anomalies on Pilot Mountain, Randolph County, North Carolina; Economic Geology, Vol. 78, pp. 605 - 617

Raines, G. L., T. W. Offield, and E. S. Santos, 1978 Remote Sensing and Subsurface Definition of Faciès and Structure Related to Uranium Deposits, Powder River Basin, Wyoming: Economic Geology Vol. 73, pp. 1706 - 1723

Reimchen, T. H. F., 1982, Location of Economic Gypsum Deposits by Integration of MuItispectral, Multitemporal, Geophysical, Geochemical, Geobotanical, and Geological Data. Proceedings of the International Symposium on Remote Sensing of Environment, Second Thematic Conference, Remote Sensing for Exploration Geology, Fort Worth, Texas, Dec. 1982, pp. 119 - 132.

Rowan, L. C. and M. S. Abrams, 1978, Evaluation of Landsat MuItispectral Scanner images for mapping altered rocks in the East Timtic Mountains, Utah: U.S. Geological Survey Open-File Rept., pp. 78 - 736, 73p.

Sabins, F. F., 1978, Remote Sensing, Principals and Interpretation, Freeman, San Fransisco, 1978

Segal, D. B., 1983, Use of LANDSAT Multispectral Scanner Data for the Definition of Limonitic Exposures in Heavily Vegetated Areas., Economic Geology, Vol.78, No. 4 June - July, 1983, pp. 711 - 722